doi:10.1246/cl.2010.1080
1080 Published on the web September 4, 2010

Photocatalytic Activity of Ni-loaded TiO_2 Nanoparticles Precisely Controlled in Size and Shape

Takeshi Kimijima, Takafumi Sasaki, Masafumi Nakaya, Kiyoshi Kanie, and Atsushi Muramatsu*
Institute of Multidisciplinary Research for Advanced Materials, Tohoku University, 2-1-1 Katahira, Aoba-ku, Sendai, Miyagi 980-8577

(Received June 29, 2010; CL-100595; E-mail: mura@tagen.tohoku.ac.jp)

Photocatalytic activity of anatase-type TiO_2 nanoparticles with different shape, prepared by gel–sol method, was evaluated. Particle morphology, that is, the main surface crystal plane was found critically decisive for the photocatalytic activity for H_2 evolution from aqueous ethanol. Namely, the activity of cubic particles bound by {100} and {001} faces, estimated from high-resolution TEM images, showed highest activity among one tested.

Anatase-type titanium oxide (TiO_2) is one of the most attractive photocatalysts because of its excellent chemical stability and high hydrogen evolution ability.[1] TiO_2 nanoparticulate catalyst has big advantages such as large surface area and/or quantum size effect.[2] Generally speaking, the catalytic performance of nanoparticles is influenced by crystal phase, size, surface area, and crystallinity.[3–6] Particles bounded by different crystal planes are well known to show different characteristic features, even if they are the same crystal system.[7–13] Therefore, the precise control in size, shape, and surface plane of nanoparticles is critically important so as to develop high-performance photocatalysts. Recently, Lu et al. have reported that micro-sized TiO_2 particles with precisely controlled size and outer surface show fivefold higher photocatalytic activity than conventional TiO_2 powder, P-25.[10,11] However, the role of particle morphology as well as the outer surface plane on the photocatalytic activity of TiO_2 nanoparticles has not been identified yet, since monodispersed TiO_2 nanoparticulate catalysts precisely controlled in size and shape have never been systematically synthesized, because of many technological barriers to obtaining well-defined TiO_2 catalyst materials. In our previous study, a gel–sol method for the synthesis of monodispersed anatase-type TiO_2 nanoparticles has been established with tailor-made size and shape.[14] In this regard, the objective of the present study is to investigate effects of morphology and surface crystal plane of anatase-type TiO_2 nanoparticles, prepared by the gel–sol method, upon the photocatalytic activity. Figure 1 shows transmission electron micrographs (TEMs) of the TiO_2 nanoparticles **T1**–**T4** precisely controlled in size and shape. The synthetic procedure of **T1**–**T4** is summarized in Supporting Information (SI).[15] **T1** is an inhomogeneous shape (Figure 1a), **T2** and **T3** are spindle-shaped TiO_2 nanoparticles with different aspect ratio (Figures 1b and 1c). **T4** has a cubic particle (Figure 1d). This morphological change resulted from the selective adsorption of the shape controller on the specific crystal plane of the TiO_2 nanoparticles.[14] The mean particle sizes as long axis with distribution of **T1**, **T2**, **T3**, and **T4** were calculated to be 26.1 ± 7.4, 38.7 ± 13.7, 205.4 ± 75.1, and 18.3 ± 4.7 nm, respectively. The aspect ratios of **T2** and **T3** were 2.4 and 5.5, respectively. Final particle size was easily controlled by seeding.[14c] In addition, the

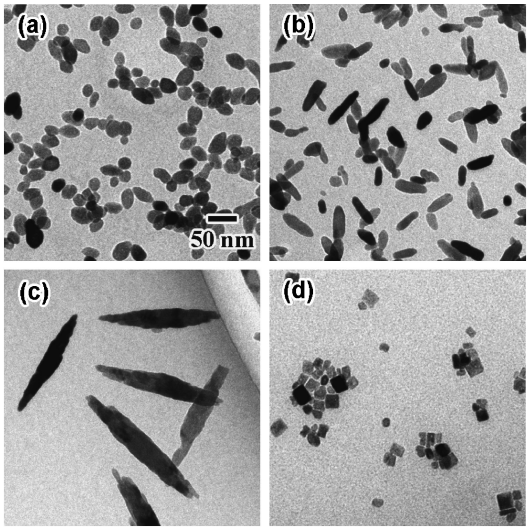

Figure 1. TEM images of TiO_2 nanoparticles obtained by the gel–sol method: (a) **T1**, inhomogeneous; (b) **T2**, spindle with the aspect ratio of 2.4; (c) **T3**, spindle with the aspect ratio of 5.5; and (d) **T4**, cubic. The scale bar in (a) is common for all images.

crystal structure of as-prepared TiO_2 nanoparticles was confirmed as anatase by X-ray diffraction (XRD) analysis without any impurity on their surfaces, as verified by X-ray photoelectron spectroscopy (see SI[15]). The XRD measurement also showed that crystallinity of **T1**–**T4** was almost the same. Then, 0.50 wt % Ni nanoparticles were uniformly loaded on **T1**–**T4** surfaces, as a cocatalyst, by liquid-phase reductive deposition.[16] Here, the nickel nanoparticles collect the photogenerated electrons and suppress the recombination of electrons and holes. The Ni-loading procedure is also illustrated in SI.[15]

Before the photocatalytic activity test, the surface crystal plane of **T1**–**T4** was investigated by high-resolution TEM (HR-TEM) analysis. Figure 2 shows HR-TEM (a, c), their magnified and fast Fourier transform (FFT) images (b, d) of **T3** and **T4**, respectively. The lattice spacing of **T3** is assigned as 0.46 nm, which was determined by the HRTEM image shown in Figure 2b. The spacing is completely consistent with a half of the unit cell length of *c* axis of the anatase crystal. Thus, it can be concluded that the lattice fringe results from the interplanar distance of (002) plane of anatase-type TiO_2. The particle was grown along the *c* axis so that the shape became a spindle, where the shape control may be due to the selective adsorption of NH_3 on the crystal plane parallel to the *c* axis.[14] As shown in Figures 2a and 2b, **T3** has {100} and {101} faces as exposed surface. The growth direction of **T2** was the same as **T3**. On the other hand, lattice spacing of **T4** is calculated to be 0.19 nm from the HRTEM image shown in Figure 2d. The lattice fringe

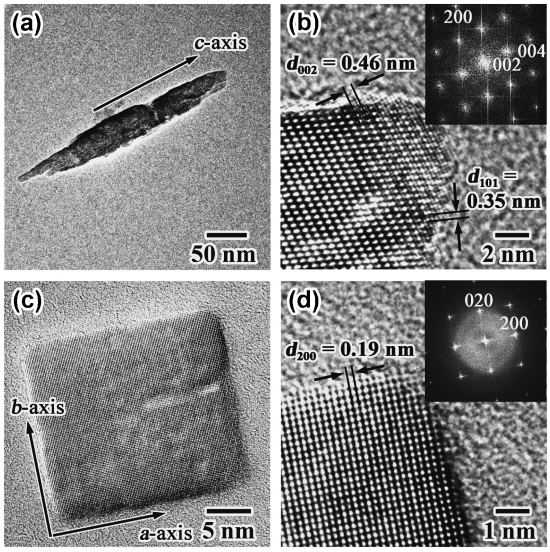

Figure 2. High-resolution TEM images of **T3** (a) and **T4** (c) shown in Figures 1c and 1d, and their high-magnified images (b, d), and the fast Fourier transform images of Figures 2b and 2d (inset).

corresponds to the interplanar distance of (200) and (020) planes of anatase-type TiO_2 because the unit cell length of the *a* axis of anatase crystal is 0.38 nm. A surface perpendicular to the *c* axis is {001} face because the FFT pattern exhibited in Figure 2d is indexed as the [001] zone axis. Judging from HRTEM and FFT analyses of **T4**, the particles were bounded by {100} and {001} faces, since the shape was controlled by the specific adsorption of sodium oleate.[14]

Photocatalytic activity of Ni-loaded **T1**–**T4** was evaluated by measuring the amount of H_2 evolution from ethanol as follows: 10.0 mg of 0.50 wt % Ni-loaded **T1**–**T4** were dispersed to 6.0 mL of 10 vol % aqueous ethanol in a quartz cell. Ni-loading was confirmed as optimum so as not to reduce the absorption of light as well as to evaluate the photocatalytic activity. After the mixture was deaerated thoroughly, irradiation by 500 W high-pressure mercury lamps without any filter was introduced to the quartz cell under vigorous stirring, where light intensity was adjusted to 0.85 W cm^{-2} and the reaction time was 3 h. The results are summarized in Figure 3. The photocatalytic activities per unit surface area of **T1**, **T2**, **T3**, and **T4** are 7.58×10^2, 2.18×10^2, 2.56×10^2, and 1.03×10^3 μL h^{-1} m^{-2}, respectively. **T4** shows the highest photocatalytic activity and exceeded **ST-01**, a conventional catalyst, and its main exposed plane is {101}.[17] So it can be concluded that this remarkably high photocatalytic activity of **T4** results from the large surface area of exposed {001} plane, compared with that of other nanoparticles. In spite of being a sheet-type catalyst, rather than particulate, the higher photocatalytic activity has been reported to confirm the specific plane, {001} due to higher density of unsaturated fivefold Ti atoms on the (001) surface.[18,19] On the other hand, the activity of **T3** is almost the same as that of **T2** in spite of its small surface area. This might be due to the same exposed {101} and {100} plane of **T2** and **T3**.

In the present report, the effect of morphology, that is, exposed crystal planes of anatase-type TiO_2 nanoparticles on the photocatalytic activity has been systematically investigated. The

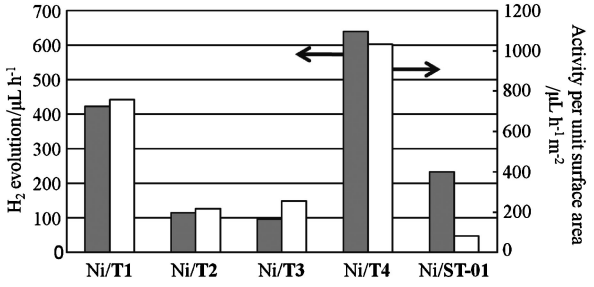

Figure 3. Photocatalytic activity of 0.50 wt % Ni-loaded size- and shape-controlled TiO_2 nanoparticles **T1**–**T4** and a conventional TiO_2 **ST-01**. Specific surface area (m^2 g^{-1}) of **T1**, **T2**, **T3**, **T4**, and **ST-01**, determined by BET method, were 55.7, 52.8, 37.4, 61.9, and 281, respectively.

Ni-loaded TiO_2 nanoparticles with a cubic morphology showed the highest photocatalytic activity for H_2 evolution from ethanolic aqueous solution. Judging from HRTEM and FFT images, the cubic TiO_2 nanoparticles were found bounded by {100} and {001} faces. Hence, {001} surface promotes H_2 evolution over the photocatalytic reaction. As a result, the precise control of morphology and crystal surface plane of nanosized particles is critically decisive for photocatalytic activity. Enhancement of photocatalytic activity of other oxides is probably achieved by control of shape and surface plane in monodispersed nanoparticles.

References and Notes

1 D. E. Scaife, *Sol. Energy* **1980**, *25*, 41.
2 H. Lin, C. P. Huang, W. Li, C. Ni, S. I. Shah, Y.-H. Tseng, *Appl. Catal., B* **2006**, *68*, 1.
3 S. Monticone, R. Tufeu, A. V. Kanaev, E. Scolan, C. Sanchez, *Appl. Surf. Sci.* **2000**, *162–163*, 565.
4 K. Y. Jung, S. B. Park, S.-K. Ihm, *Appl. Catal., A* **2002**, *224*, 229.
5 H. Kominami, T. Matsuura, K. Iwai, B. Ohtani, S. Nishimoto, Y. Kera, *Chem. Lett.* **1995**, 693.
6 W. Tang, Z. Chen, S. Katoh, *Chem. Lett.* **2004**, *33*, 1200.
7 D. Zhang, G. Li, X. Yang, J. C. Yu, *Chem. Commun.* **2009**, 4381.
8 T. Ohno, K. Sarukawa, M. Matsumura, *New J. Chem.* **2002**, *26*, 1167.
9 E. Bae, N. Murakami, T. Ohno, *J. Mol. Catal. A: Chem.* **2009**, *300*, 72.
10 H. G. Yang, C. H. Sun, S. Z. Qiao, J. Zou, G. Liu, S. C. Smith, H. M. Cheng, G. Q. Lu, *Nature* **2008**, *453*, 638.
11 H. G. Yang, G. Liu, S. Z. Qiao, C. H. Sun, Y. G. Jin, S. C. Smith, J. Zou, H. M. Cheng, G. Q. Lu, *J. Am. Chem. Soc.* **2009**, *131*, 4078.
12 J.-Y. Ho, M. H. Huang, *J. Phys. Chem. C* **2009**, *113*, 14159.
13 F. Amano, O.-O. Prieto-Mahaney, Y. Terada, T. Yasumoto, T. Shibayama, B. Ohtani, *Chem. Mater.* **2009**, *21*, 2601.
14 a) T. Sugimoto, X. Zhou, A. Muramatsu, *J. Colloid Interface Sci.* **2002**, *252*, 339. b) T. Sugimoto, X. Zhou, *J. Colloid Interface Sci.* **2002**, *252*, 347. c) T. Sugimoto, X. Zhou, A. Muramatsu, *J. Colloid Interface Sci.* **2003**, *259*, 43. d) T. Sugimoto, X. Zhou, A. Muramatsu, *J. Colloid Interface Sci.* **2003**, *259*, 53. e) T. Sugimoto, K. Okada, H. Itoh, *J. Colloid Interface Sci.* **1997**, *193*, 140.
15 Supporting Information is available electronically on the CSJ-Journal Web site, http://www.csj.jp/journals/chem-lett/index.html.
16 H. Takahashi, Y. Sunagawa, S. Myagmarjav, A. Muramatsu, *Catal. Surv. Asia* **2005**, *9*, 187.
17 P. Wen, H. Itoh, W. Tang, Q. Feng, *Langmuir* **2007**, *23*, 11782.
18 X.-Q. Gong, A. Selloni, *J. Phys. Chem. B* **2005**, *109*, 19560.
19 U. Diebold, *Surf. Sci. Rep.* **2003**, *48*, 53.

